

# Analyst

Accepted Manuscript



This is an *Accepted Manuscript*, which has been through the Royal Society of Chemistry peer review process and has been accepted for publication.

*Accepted Manuscripts* are published online shortly after acceptance, before technical editing, formatting and proof reading. Using this free service, authors can make their results available to the community, in citable form, before we publish the edited article. We will replace this *Accepted Manuscript* with the edited and formatted *Advance Article* as soon as it is available.

You can find more information about *Accepted Manuscripts* in the [Information for Authors](#).

Please note that technical editing may introduce minor changes to the text and/or graphics, which may alter content. The journal's standard [Terms & Conditions](#) and the [Ethical guidelines](#) still apply. In no event shall the Royal Society of Chemistry be held responsible for any errors or omissions in this *Accepted Manuscript* or any consequences arising from the use of any information it contains.

1  
2  
3  
4  
5  
6  
7  
8  
9  
10  
11 **Extremely supercharged proteins in mass spectrometry: Profiling the pH of electrospray**  
12 **generated droplets, narrowing charge state distributions, and increasing ion fragmentation**  
13  
14  
15  
16  
17  
18  
19

20 Muhammad A. Zenaidee and William A. Donald

21 *School of Chemistry, University of New South Wales, Sydney, New South Wales, Australia, 2052*  
22  
23  
24  
25  
26

27 For submission to *The Analyst*  
28  
29  
30  
31  
32  
33  
34  
35  
36  
37  
38  
39  
40  
41  
42  
43  
44  
45  
46  
47

48 Address reprint requests to:  
49

50 William A. Donald  
51 Dalton Building 221  
52 School of Chemistry  
53 The University of New South Wales  
54 Sydney, New South Wales 2052  
55 Australia  
56 Phone: +61(2) 9385 8827  
57 FAX: +61(2) 9385 6141  
58 [w.donald@unsw.edu.au](mailto:w.donald@unsw.edu.au)  
59  
60

**Abstract**

The effects of 12 acids, 4 solvents, and 8 low-volatility additives that increase analyte charging (*i.e.*, superchargers) on the charge state distributions (CSDs) of protein ions in ESI-MS were investigated. We discovered that (i) relatively low concentrations [5 %(v/v)] of 1,2-butylene carbonate (and 4-vinyl-1,3-dioxolan-2-one) can be added to ESI solutions to form higher charge states of cytochrome *c* and myoglobin ions than by using more traditional additives (*e.g.*, propylene carbonate, sulfolane, or *m*-nitrobenzyl alcohol) under these conditions and (ii) the width of CSDs narrow as the effectiveness of superchargers increase, which concentrates protein ions into fewer detection channels. The use of strong acids ( $pK_a$  values  $< 0$ ) results in essentially no protein supercharging, higher adduction of acid molecules, and wider CSDs for many superchargers and proteins, whereas the use of weak acids ( $pK_a > 0$ ) results in significantly higher protein ion charging, less acid adduction, and narrower CSDs, indicating that protein ion supercharging in ESI can be significantly limited by the binding of conjugate base anions of acids that neutralize charge sites and broaden CSDs. The extent of protein charging as a function of acid identity (HA) does not strongly correlate with gas-phase proton transfer data (*i.e.*, gas-phase basicity and proton affinity values for HA and  $A^-$ ), solution-phase protein secondary structures (as determined by circular dichroism spectroscopy), and/or acid molecule volatility data. For protein-denaturing solutions, these data were used to infer that the “effective” pH of ESI generated droplets near the moment of ion formation can be  $\sim 0$ , which is *ca.* 1 to 3 pH units lower than the pH of the solutions prior to ESI. Electron capture dissociation (ECD) of [ubiquitin, 17H] $^{17+}$  resulted in the identification of 223 cleavages, 74 of 75 inter-residue sites, and 92% ECD fragmentation efficiency, which correspond to highest of these values that have been obtained by ECD of a single isolated charge state of ubiquitin.

## Table of Contents Graphic

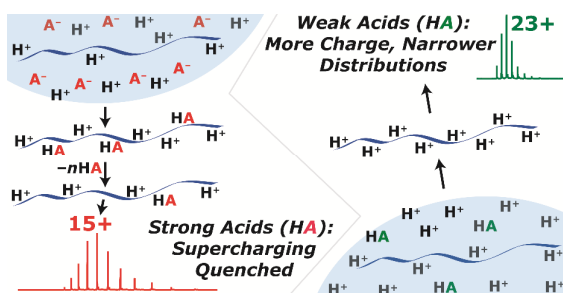


## Table of Contents Entry

High-performance solutions for supercharging proteins in electrospray ionization were optimized and the origin of the strong dependence of supercharging on acid strength was investigated

**Running title:** Extremely supercharged protein ions

**Keywords:** Electrospray ionization, mass spectrometry, electron capture dissociation, protein, supercharging, supercharger, 1,2-butylene carbonate, propylene carbonate, ethylene carbonate, *m*-nitrobenzyl alcohol, sulfolane

## Introduction

Electrospray ionization (ESI) is effective for forming intact gaseous ions of proteins from solution for detection by mass spectrometry (MS).<sup>1</sup> A distinctive advantage of ESI is that a distribution of multiply charged ions,  $[M, zH]^{z+}$  (charge state distributions; CSDs), can be produced that have higher charge densities than those formed using other known methods. Multiple charging extends the mass range of most mass analysers,<sup>1</sup> which enables protein ions to be detected using nearly any ESI mass spectrometer. Ions that have more charges tend to dissociate significantly more readily than those with fewer charges partly because charge sites often direct the bond cleavage of ions in many types of tandem-MS experiments.<sup>2</sup> For electron capture dissociation (ECD), the number of fragment ions,<sup>3</sup> the efficiency of fragmentation,<sup>3</sup> and the amount of energy that is deposited increases as ion charge increases,<sup>3a,b,4</sup> which can significantly increase the number of cleavage sites and the resulting sequence coverage. ESI solutions that denature proteins are often used to ensure the formation of protein ions in elongated conformations that hold significantly more charge than those that are compact.<sup>5</sup> However, the widths of protein CSDs increase significantly as the size of proteins increase, which reduces signal-to-noise ratios ( $S/N$ ) by distributing signal over more detection channels and “clutters” mass spectra.<sup>6</sup> The  $S/N$  for protein ions formed from denaturing solutions decrease exponentially as protein sizes increase owing solely to CSD broadening.<sup>6</sup> Thus, it would be useful to (i) narrow protein CSDs and (ii) shift charge states to low  $m/z$  values where many MS instruments excel.

The dynamic processes that occur during ESI are complex and many factors affect protein CSDs (*e.g.*, pH,<sup>7</sup> conformation,<sup>5,7</sup> proton transfer reactivity,<sup>8</sup> and surface tension).<sup>9</sup> In ESI, a potential is applied to a solution flowing through a capillary, which results in the emission of a fine mist of charged droplets.<sup>1</sup> The surface charge density of the droplets increases as relatively volatile components of the droplets preferentially evaporate. If sufficiently high, charge-charge repulsion can overcome the forces that hold droplets together at the Rayleigh limit,<sup>1</sup> in which the number of charges a droplet can accommodate scales with  $\gamma^{1/2}$  (where  $\gamma$  is surface tension). Upon droplet fission, a stream of smaller droplets is emitted that removes a significant fraction of charge (*ca.* 10

1 to 50%), but relatively little mass ( $\ll 5\%$ ) from the precursor.<sup>1,10</sup> In the charge residue model,<sup>11</sup>  
2 sequential evaporation/fission cycles yield a droplet containing a single ion that evaporates. In the  
3 ion evaporation model,<sup>12</sup> an ion desorbs from a droplet that is sufficiently charged. Over the  
4 lifespan of an ESI droplet, the vast majority of droplet mass is lost to evaporation,<sup>1</sup> which results in  
5 the enrichment of charge carriers (*e.g.*,  $\text{H}_3\text{O}^+$ ). Based on laser-induced fluorescence measurements,  
6 the pH of positively charged droplets decrease by  $\geq 1$  pH unit during ESI,<sup>13</sup> which is consistent with  
7 results for the dissociation of pH sensitive metal ion complexes in ESI-MS.<sup>14</sup> However, the pH of  
8 ESI generated droplets that contain protein ions is not known.

9  
10  
11  
12  
13  
14  
15  
16  
17  
18  
19  
20  
21  
22  
23  
24  
25  
26  
27  
28  
29  
30  
31  
32  
33  
34  
35  
36  
37  
38  
39  
40  
41  
42  
43  
44  
45  
46  
47  
48  
49  
50  
51  
52  
53  
54  
55  
56  
57  
58  
59  
60  
In ESI, the extent that proteins are charged depends on the protein structure (*e.g.*, number of  
basic sites),<sup>7,15</sup> the solution composition,<sup>9,16</sup> and instrumental effects.<sup>17</sup> The apparent gas-phase  
basicity values ( $\text{GB}^{\text{app}}$ , which include the repulsive Coulomb barrier to proton transfer) of protein  
ions decrease as the charge states increase.<sup>18</sup> If sufficiently protonated, the  $\text{GB}^{\text{app}}$  values of protein  
ions approach the GB values of solvent molecules, which can result in proton transfer reactions  
between protein ions and residual solvent that can limit protein ion charging.<sup>8a,18a</sup> For example, the  
average charge states of cytochrome *c* (cyt *c*) ions formed from solutions containing 47/50/3%  
water/solvent/acetic acid (solvent = water, GB of 157.7 kcal/mol; methanol, 173.2 kcal/mol;  
acetonitrile, 179.0 kcal/mol; isopropanol, 182.3 kcal/mol) steadily decreased from 16.8 (water) to  
15.6 (isopropanol) as the GB of the solvent increased.<sup>8a</sup>

The neutralization of protonation sites by the adduction of anions in ESI can also reduce  
analyte charging. For example, the average charge states of protonated cyt *c* ions formed by ESI  
from denaturing solutions can shift by up to *ca.* 15% by using different acids (*e.g.*, 14.8 vs. 12.5, for  
 $\text{CH}_3\text{COOH}$  vs.  $\text{CCl}_3\text{COOH}$ ),<sup>16</sup> which indicates that the conjugate base anions of the acids can  
neutralize protein charge states. The binding of an anion to a protonation site reduces the charge of  
the protein ion by forming a neutral acid adduct ( $[\text{M}, (z-1)\text{H}, \text{HA}]^{(z-1)+}$ ) that can be readily lost.<sup>16</sup>  
Acid/anion adduction to other biomolecules has been observed in ESI.<sup>16,19</sup> Although the role of  
anions/solvent molecules in reducing analyte charging in ESI is recognized, the reported shifts in  
the CSDs as a result of changing the identity of anions/solvent in ESI solutions are relatively

1 modest (*e.g.*,  $\leq 3$  protons for cyt *c* ions).<sup>16</sup>

2  
3 Protein ion charge states can be shifted to higher values by chemical derivatization,<sup>20</sup>  
4 altering ESI source conditions,<sup>17b</sup> and modifying the composition of ESI solutions<sup>19a</sup> and plumes.<sup>21</sup>  
5  
6 A simple approach to form protein ions in the highest known protonation states is to add small non-  
7 volatile molecules (superchargers, SCs) that are polar and have relatively high  $\gamma$  values into ESI  
8 solutions.<sup>8a,9a,22</sup> More than a dozen SCs have been used to significantly increase the extent of  
9 analyte charging in ESI,<sup>8a,9a,22</sup> including *m*-nitrobenzyl alcohol (*m*-NBA)<sup>9a</sup> and sulfolane.<sup>22a,23</sup>  
10  
11 Supercharging additives are useful for significantly increasing tandem-MS ion fragmentation  
12 efficiency and the resulting sequence coverage<sup>24</sup> for proteins and peptides in liquid chromatography  
13 ESI-MS experiments.<sup>25</sup>  
14  
15

16  
17 Three mechanisms have been proposed for protein supercharging in ESI from denaturing  
18 solutions,<sup>9a,23,26</sup> in which protein conformational effects should be negligible. For all three, non-  
19 volatile supercharging additives are enriched during sequential droplet evaporation/fission  
20 cycles.<sup>22b,27</sup> In the surface-tension mechanism,<sup>9a</sup> the additives increase the droplet  $\gamma$  near the  
21 moment of ion formation to form more highly charged droplets than without the additive, which  
22 results in the transfer of more charge to the analyte. However, the role of  $\gamma$  in ESI has been  
23 questioned<sup>22a,28</sup> owing partly to the many factors that can affect protein ion CSDs, which makes it  
24 challenging to determine the dominant factors that are responsible for the extent of protein charging  
25 in ESI. For example, Samalikova *et al.* suggested that  $\gamma$  in ESI is not a significant factor based  
26 partly on the observation that protein CSDs did not shift upon use of ESI solutions that were  
27 acidified with HCl compared to acetic acid<sup>28</sup> because the difference in droplet  $\gamma$  values were  
28 predicted to be relatively large (~60%). However, the neutralization of protonation sites by the  
29 conjugate base anions of acids did not appear to be considered. In the Brønsted-acid/base  
30 mechanism,<sup>26</sup> the enhanced charging of analytes by the addition of SCs is attributed to protonated  
31 supercharging additives being less basic than water, which ultimately results in the formation of  
32 more highly protonated analyte molecules. In the dipole-moment based mechanism,<sup>23</sup> supercharging  
33 additives solvate protonation sites in mature ESI droplets, which decreases charge-charge repulsion  
34  
35  
36  
37  
38  
39  
40  
41  
42  
43  
44  
45  
46  
47  
48  
49  
50  
51  
52  
53  
54  
55  
56  
57  
58  
59  
60

1 and increases the number of charges accommodated by an analyte ion.

2  
3 Recently, we discovered that by use of ethylene carbonate (EC) and propylene carbonate  
4 (PC),<sup>29</sup> significantly higher charge states of several protein ions can be formed than had been  
5 reported by use of *m*-NBA, sulfolane, and other supercharging additives. For example, by addition  
6 of 15% PC to solutions containing 44/54/1 methanol/water/acetic acid and 10  $\mu$ M of cyt *c*, the  
7 average and highest observed charge states increased from  $15.7 \pm 0.1$  and 21+ (no additive) to  $21.9$   
8  $\pm 0.8$  and 26+ (PC), which was significantly higher than by the use of 0.5% *m*-NBA ( $17.8 \pm 0.2$  and  
9 24+) and 1% sulfolane ( $18.7 \pm 0.4$  and 24+).<sup>29</sup> EC can be used to shift nearly the entire CSDs of cyt  
10 *c* ions to higher charge states than the theoretical maximum limit that is based on proton transfer  
11 reactivity with the most basic solvent (methanol; 16+).<sup>18a,29</sup> Although relatively high concentrations  
12 of PC/EC were required to form “extremely” supercharged proteins,<sup>29</sup> these additives can be useful  
13 for narrowing CSDs.  
14  
15

16  
17 Here, we report that 1,2-butylene carbonate (BC) and 4-vinyl-1,3-dioxalan-2-one (4V) can  
18 be added to ESI solutions at relatively low concentrations [5%(v/v)] to form protein ions in  
19 significantly higher charge states than by use of PC. The role of different additives (8 supercharging  
20 molecules, 12 acid molecules and 4 solvent molecules) on protein ion CSDs formed in ESI-MS was  
21 investigated. The extent of protein supercharging in ESI was strongly dependent on the strength the  
22 acid (*i.e.*, CSDs can shift by nearly 10 protons by using different acids), indicating that the extent of  
23 protein supercharging in ESI can be significantly limited by the binding of anions during ESI.  
24  
25

## 26 27 28 29 30 31 32 33 34 35 36 37 38 39 40 41 42 43 **Methods**

44  
45 For ESI-MS experiments, a linear quadrupole ion trap MS (LTQ-MS; Thermo Scientific)  
46 was used. ESI solutions were infused into the ESI source (3  $\mu$ l/min) and ions were formed by  
47 applying a voltage of +3 to 4.5 kV to the ESI capillary relative to the capillary MS inlet (250-450  
48  $^{\circ}$ C; Table S1). ESI solutions contained 5  $\mu$ M protein, 5%(v/v) supercharger, 0.5% acetic acid and  
49 94.5% distilled water (18 M $\Omega$  Milli-Q water), unless stated otherwise. All proteins, acids,  
50 supercharging additives, and organic solvents were obtained from commercial sources  
51 (Supplementary Information; SI). For ECD and high-resolution MS, a hybrid LTQ-MS and 7 T  
52  
53  
54  
55  
56  
57  
58  
59  
60



1 Fourier transform ion cyclotron resonance MS (LTQ-FT/ICR-MS; Thermo Scientific) was used.  
2  
3 Charge states were mass selected in the LTQ-MS ( $\pm 5$   $m/z$  isolation window), thermalized by  
4  
5 collisions with He(g) buffer gas ( $\sim 1$  mTorr),<sup>30</sup> and transferred to the FT-ICR for ECD (25 ms  
6  
7 irradiation time; 3 eV initial energy). The automatic gain control was used to ensure that the ion trap  
8  
9 was not overloaded (10 ms maximum ion accumulation time). ESI mass spectra were collected in  
10  
11 triplicate and the uncertainty values were approximated by the standard deviation of these replicates  
12  
13 ( $\pm 1$  standard deviation). Details of (i) circular dichroism, pH, and surface tension measurements;  
14  
15 and (ii) the CD spectral analysis, and methods for calculating the average charge states ( $\langle z \rangle$ ), CSD  
16  
17 widths ( $W_z$ ; full-width at half max), electron capture efficiencies, fragmentation efficiencies, and  
18  
19 sequence coverage are given in the SI.  
20  
21

## 22 Results and Discussion

23  
24  
25 *Additive performance.* Representative ESI mass spectra of aqueous solutions containing 5  
26  
27  $\mu\text{M}$  cyt *c*, 0.5% acetic acid, and either no additional additive or one of seven different solution  
28  
29 additives (BC, 4V, PC, 1,4-butanedisulfone, sulfolane, *m*-NBA, and 1,3-propanedisulfone) at “optimal”  
30  
31 concentrations for maximising protein charging are shown in Figure 1. The most abundant, the  
32  
33 highest observed, and the average charge states of cyt *c* ions formed by use of each additive (*i.e.*,  
34  
35 performance characteristics of supercharging) are shown in Table 1. By addition of any of these  
36  
37 seven reagents, the CSD of cyt *c* ions increased from an average charge state of  $14.7 \pm 0.1$  (no  
38  
39 additive) to values that range from  $16.5 \pm 0.1$  (1,3-propanedisulfone) to  $22.6 \pm 0.1$  (4-vinyl-1,3-  
40  
41 dioxolan-2-one). By addition of 5%(v/v) BC (or 4V), significantly higher charge states were formed  
42  
43 than by use of the more traditional supercharging additives, PC,<sup>29</sup> sulfolane,<sup>22a</sup> and *m*-NBA<sup>22c</sup> under  
44  
45 these conditions (Table 1). For example, by addition of BC, the average and maximum charge states  
46  
47 were a respective  $22.6 \pm 0.2$  and 26+, which was higher than the corresponding values for PC ( $21.8$   
48  
49  $\pm 0.2$ , 25+), sulfolane ( $19.4 \pm 0.3$ , 23+), and *m*-NBA ( $17.4 \pm 0.2$ , 22+; 3% is near the solubility limit  
50  
51 in acidified water).  
52  
53  
54

55  
56 For myoglobin, which is more acidic (pI *ca.* 7) than cyt *c* (pI *ca.* 10 to 11),<sup>31</sup> addition of 5%  
57  
58 BC increased the average and highest observed charge states of protonated myoglobin from  $20.6 \pm$   
59  
60

0.5 and 28+ (no additive) to  $30.7 \pm 0.1$  and 34+ (Table 1); *i.e.*, a 50% increase in the average charge states ( $\sim 10.1$  protons). In contrast, the extent of myoglobin charging was lower by use of PC ( $29.8 \pm 0.3$  and 32+), sulfolane ( $26.1 \pm 0.1$  and 30+), and *m*-NBA ( $24.7 \pm 0.6$  and 30+). That is, BC (and 4V) can be used to form the highest known protonation states of cytochrome *c* and myoglobin (to our knowledge).

*Effects of superchargers on CSDs.* Based on these results, the relative order of supercharger effectiveness was (Table 1):

BC  $\approx$  4V > PC > EC > 1,4-butanedisulfone > sulfolane > *m*-NBA > 1,3-propanedisulfone

Interestingly, as the effectiveness of protein superchargers increased, the width of the protein CSDs tended to narrow (Table 1). For example, the  $W_z$  values of the CSDs of myoglobin steadily decreased from  $5.9 \pm 1.7$  to  $1.7 \pm 0.2$  as the extent of charging increased from  $\langle z \rangle = 20.9 \pm 0.2$  (1,3-propanedisulfone) to  $\langle z \rangle = 30.6 \pm 0.2$  (4V). The origin of the CSD narrowing is not well understood. This effect might result from the presence of supercharging additives: (i) reducing the extent that protonation sites are neutralized by anion binding within droplets near the moment of ion formation, (ii) resulting in the formation mature ESI droplets that are more homogeneous with respect to size and composition, (iii) resulting in more homogeneous conformational distributions of proteins near the moment of ion formation. The difference in the rate of proton transfer to residual solvent molecules between adjacent charge states may be significantly larger at very high charge densities than at lower charge densities, which could also contribute to CSD narrowing.<sup>8a,32</sup>

BC, 4V, 1,4-butanedisulfone and 1,3-propanedisulfone, which have not been used as ESI additives previously, were selected because they are chemical derivatives of known SCs and because these additives have relatively high surface tension values ( $> 35$  mN/m) and/or dipole moment values (*i.e.*, properties that are implicated in enhancing analyte charging in ESI; Table S2).<sup>9a,23</sup> Although the extent of protein ion charging (Table 1) from these solutions does not strongly correlate with surface tension and/or dipole moment values for this limited set of SC additives, the surface tension and dipole moment values are relatively high and should be comparable to the surface tension of water that contains a significant fraction of acetic acid, which

1 is less volatile than water. For example, the surface tension of aqueous solutions containing acetic  
2 acid decrease from 51.4 to 41.2 mN/m as the acetic acid concentrations increase from 10 to 30  
3  
4  
5  
6  
7  
8  
9  
10  
11  
12  
13  
14  
15  
16  
17  
18  
19  
20  
21  
22  
23  
24  
25  
26  
27  
28  
29  
30  
31  
32  
33  
34  
35  
36  
37  
38  
39  
40  
41  
42  
43  
44  
45  
46  
47  
48  
49  
50  
51  
52  
53  
54  
55  
56  
57  
58  
59  
60

is less volatile than water. For example, the surface tension of aqueous solutions containing acetic acid decrease from 51.4 to 41.2 mN/m as the acetic acid concentrations increase from 10 to 30 % (m/m).<sup>33</sup> These surface tension values are lower than aqueous mixtures composed of 50% (62.5 mN/m) to 90% sulfolane (50.9 mN/m), which is significantly less volatile than water.<sup>33</sup> Because protein ion charging depends on a number of factors and the precise compositions of the droplets at the moment of ion formation are not well defined, identifying the primary effects that are responsible for increasing analyte supercharging in ESI is challenging.

*Effects of acid identity.* Representative mass spectra of aqueous solutions containing 5  $\mu\text{M}$  cyt *c*, 5% 4V, and 0.5% of either acetic, iodic, nitric, or hydroiodic, or no acid are show in Figure 2. Surprisingly, the identity of the acid has a dramatic effect on the extent of protein charging and the extent of acid adduction in ESI (*i.e.*, formation of [cyt *c*, *n*HA, *z*H]<sup>*z+*</sup>). For example, by use of CH<sub>3</sub>COOH and HIO<sub>3</sub> (weak acids), relatively high protein charge densities are obtained ( $\langle z \rangle = 22.7 \pm 0.4$  and  $20.6 \pm 0.2$ , respectively) and the vast majority of the protein ion signal is assigned to [cyt *c*, *z*H<sup>+</sup>]<sup>*z+*</sup> (>90%); that is, acid adduction is minimal and analyte charging is relatively high. In contrast, by use of HNO<sub>3</sub> or HI (strong acids), the average charge states are nearly ten protons lower than by use of the weak acids and the vast majority of the protein ion signal (>65%) is assigned to acid adducted protonated cyt *c*, [cyt *c*, *n*HA, *z*H]<sup>*z+*</sup> ( $n \geq 1$ ). Moreover, the extent of charging with the strong acids ( $\langle z \rangle = 14.8 \pm 0.3$  and  $14.2 \pm 0.2$  for HNO<sub>3</sub> and HI acid, respectively) is only slightly higher than that obtained by not including any acid at all ( $\langle z \rangle = 12.9 \pm 0.5$ ; Figure 2e). The use of the strong acids results in broader CSDs ( $W_z = 2.7 \pm 0.1$  and  $2.5 \pm 0.1$  for HNO<sub>3</sub> and HI acids) than by use of the weak acids ( $W_z = 1.3 \pm 0.2$  and  $1.5 \pm 0.1$  for HIO<sub>3</sub> and acetic acid).

The average charge states of [cyt *c*, *z*H]<sup>*z+*</sup> that were formed upon ESI of solutions containing 5  $\mu\text{M}$  cyt *c*, 0.5% of acid (HA = HI, HClO<sub>4</sub>, HCl, H<sub>2</sub>SO<sub>4</sub>, HNO<sub>3</sub>, HIO<sub>3</sub>, H<sub>2</sub>C<sub>2</sub>O<sub>4</sub>, H<sub>3</sub>PO<sub>4</sub>, HCOOH, C<sub>6</sub>H<sub>5</sub>COOH, CH<sub>3</sub>COOH, and C<sub>6</sub>H<sub>5</sub>OH), and either no other additive or 5% of a supercharger (4V, 1,4-butanedisulfone, sulfolane, and 1,3-propanedisulfone) are plotted as a function of acid  $\text{p}K_a$  in Figure 3. Significantly higher charge states were formed by use of any of the 7 weak acids ( $\text{p}K_a > 0$ ) than by use of any of the 5 strong acids ( $\text{p}K_a < 0$ ) for each of the four superchargers that were

1 investigated (Figure 3b-e). For example, by addition of 1,3-propanesultone, the average charge  
2 states of cyt *c* were between 16.5 and 14.5 for any of the of seven weak acids. For the strong acids,  
3 these values were between 13.2 and 12.4, which were nearly the same as that for the control  
4 solution that did not include any supercharging additive ( $\langle z \rangle = 13.1 \pm 0.1$ ). For the more effective  
5 SCs, the average charge states of cyt *c* increased by an average of 8.6 (4V), 7.5 (sulfolane), and 7.1  
6 (1,4-butanedisulfone) by using any of the 7 weak acids compared to any of the 5 strong acids. That is,  
7 the effectiveness of different SCs for enhancing analyte charging in ESI is significantly higher by  
8 use of weak acids than strong acids.

9  
10  
11  
12  
13  
14  
15  
16  
17  
18  
19  
20  
21  
22  
23  
24  
25  
26  
27  
28  
29  
30  
31  
32  
33  
34  
35  
36  
37  
38  
39  
40  
41  
42  
43  
44  
45  
46  
47  
48  
49  
50  
51  
52  
53  
54  
55  
56  
57  
58  
59  
60  
The extent of acid adduction (*i.e.*, relative formation of [cyt *c*, HA, zH]<sup>z+</sup> vs. [cyt *c*, zH]<sup>z+</sup>) is significantly higher for cyt *c* ions formed from solutions that contain strong acids than those that contain weak acids (Figure 3h-k). For example, by use of 0.5% of any of the 5 strong acids and 5% of 1,3-propanedisulfone, the relative formation of [cyt *c*, HA, zH]<sup>z+</sup> is between 57 and 77% (an average of  $68.6 \pm 7.8\%$ ). In contrast, by use of any of the 7 weak acids, the extent of acid adduction is  $\leq 30\%$ . Adduction of strong acids vs. weak acids is also dramatically higher for cyt *c* ions formed from solutions that contain the other three more effective supercharging additives (Figures 3e-h); *i.e.*, this effect is relatively general. Acid adduction can decrease with increasing analyte charge density owing to the increased energy deposited into more highly charged ions than lower charged ions, which should result in the loss of neutral HA molecules.<sup>16</sup>

*Effects of acid concentration.* The average charge states, CSD widths, and extent of acid adduction of protonated cytochrome *c* as a function of acid concentration for aqueous solutions containing 5  $\mu\text{M}$  cytochrome *c*, 5% BC and between 0.5% to 5% of either acetic acid (weak acid) or hydrochloric acid (strong acid; 0.5 to 2.5%) are shown in Table S3. As the concentration of acetic acid increased from 0.5 to 5%, the average charge state of protonated cytochrome *c* monotonically decreased from  $22.6 \pm 0.2$  to  $16.6 \pm 0.1$ , the CSDs broadened from  $W_z$  values of  $1.6 \pm 0.2$  to  $3.5 \pm 0.8$ , and the extent of acid adduction increased from  $7.3 \pm 1.0$  to  $38.9 \pm 5.1\%$  (Table S3). For HCl, as the acid concentration increased from 0.5% to 2.5%, the average charge states decreased monotonically from  $13.6 \pm 0.1$  to  $11.8 \pm 0.1$ , the widths of the CSDs broadened from  $W_z$  values of

1 2.7 ± 0.1 to 4.2 ± 0.7, and the extent of acid adduction slightly increased or stayed the same from  
2  
3 71.2 ± 3.2 to 87.6 ± 10.3 (Table S3); *i.e.*, significantly higher analyte charge densities were formed  
4  
5 by use of the weak acid (acetic acid) than the strong acid (HCl), including by use of acetic acid  
6  
7 concentrations [% (v/v)] that were a factor of 5 higher (or lower) than that of HCl under these  
8  
9 conditions. These results indicate that the strong dependence of protein supercharging by use of  
10  
11 strong compared to weak acids (Figures 3 and 4) does not result from differences in the initial molar  
12  
13 concentrations of the acids. Because the extent of charging decreases, the extent of acid adduction  
14  
15 increases, and the charge states broaden as the concentration of HCl and acetic acid increases, these  
16  
17 data are consistent with the neutralization of protein protonation sites by the binding of conjugate  
18  
19 base anions of the acids limiting the extent of protein supercharging in ESI.  
20  
21

22  
23 *Other correlations?* Recently, the extent of protonated protein ion charging by use of  
24  
25 nitrophenol and sulfolane was reported to be limited by ion-pairing (*i.e.*, the formation of anion  
26  
27 adduction to protonated analytes),<sup>26</sup> which was rationalized by using the best-match gas-phase  
28  
29 basicity model for positively charged analytes in relatively low charge states that are relatively  
30  
31 basic.<sup>34</sup> In this model, R-NH<sub>2</sub>···H<sup>+</sup>···A<sup>-</sup> interactions (where R-NH<sub>2</sub> is a basic site and A<sup>-</sup> is an anion)  
32  
33 will be most favourable if the apparent GB of the amine is close to that of the GB of the anion.<sup>34</sup> In  
34  
35 our experiments, similar extents of acid adduction were observed by use of perchloric acid [GB(A<sup>-</sup>)  
36  
37 = 1200 kJ/mol; strong acid] and HCl [GB(Cl<sup>-</sup>) = 1374 kJ/mol; strong acid].<sup>35</sup> However, the GB  
38  
39 values differ by 174 kJ/mol (Figure S1). Moreover, the GB of Cl<sup>-</sup> is 23 and 51 kJ/mol *higher* than  
40  
41 those for H<sub>2</sub>PO<sub>4</sub><sup>-</sup> and HC<sub>2</sub>O<sub>4</sub><sup>-</sup>,<sup>35</sup> respectively, and the extent of acid adduction values by use of  
42  
43 H<sub>3</sub>PO<sub>4</sub> and H<sub>2</sub>C<sub>2</sub>O<sub>4</sub> (weak acids) were significantly lower than that for HCl. That is, the extent of  
44  
45 protein ion charging did not correlate with the GB values of the anions (Figure S1). The GB values  
46  
47 of the 12 conjugate base anions in our experiments range from 1200 kJ/mol (ClO<sub>4</sub><sup>-</sup>) to 1432 kJ/mol  
48  
49 (deprotonated phenol). Williams and co-workers have measured the apparent GB of protonated  
50  
51 cytochrome *c* ions,<sup>18b</sup> which decreased from 980 kJ/mol (3+) to 801 kJ/mol (15+) as charge states  
52  
53 increased; *i.e.*, the GB<sup>app</sup> values of protonated cytochrome *c* ions are more than 200 kJ/mol lower  
54  
55 than the GB of the least basic anion of the 12 acids investigated. The difference between the GB of  
56  
57  
58  
59  
60

1 the anions and the  $GB^{app}$  of the protein ions should continue to increase as the charge states increase  
2 because Coulomb repulsion will increase and the number of basic sites that are available for  
3 protonation will decrease as charge states increase. Given the large difference in GB and  $GB^{app}$   
4 values between the 12 anions and extensively protonated protein ions ( $> 200$  kJ/mol), it is not  
5 expected that the GB of the anions should necessarily correlate with the extent of protein ion  
6 charging and acid adduction based on the matching GB model for protonated protein ions in  
7 relatively low charge states. In addition, the extent of cyt *c* charging as a function of acid identity  
8 (Figure 3) did not strongly correlate with (i) the proton affinity (PA) values of the conjugate base  
9 anions of the acids ( $A^-$ ); and (ii) the GB/PA of the neutral acids (Figure S1).

10  
11  
12  
13  
14  
15  
16  
17  
18  
19  
20  
21 The relative difference in the extent of protein ion charging (and extent of acid adduction)  
22 by use of strong acids compared to weak acids did not correlate with acid volatility (*e.g.*, Henry's  
23 Law constants, boiling points, and/or vapour pressures; Figure S2 and Table S4). For example, the  
24 boiling point and Henry's law constant for HCl (strong acid) are  $-85$  °C and  $1.5 \times 10^1$  mol  $m^{-3}$  Pa $^{-1}$   
25 and those for benzoic acid are  $249$  °C and  $2.9 \times 10^2$  mol  $m^{-3}$  Pa $^{-1}$ , respectively. The average charge  
26 states and extent of acid adduction for cytochrome *c* by use of benzoic acid is  $21.5 \pm 0.3$  and  $13.2 \pm$   
27  $1.9$  %, whereas that for HCl is  $13.6 \pm 0.1$  and  $71.2 \pm 3.2$  %. These data suggest that the acids do not  
28 necessarily need to be non-volatile (or volatile) to effectively quench protein supercharging.

29  
30  
31  
32  
33  
34  
35  
36  
37  
38  
39  
40 In solution, different anions can destabilize protein structure to different extents (*i.e.*,  
41 Hofmeister effects).<sup>36</sup> Williams and co-workers determined that the extent of "electrothermal"  
42 supercharging of proteins from native solutions (increasing protein charging by increasing the  
43 electric field between the ESI capillary and the capillary entrance to the mass spectrometer) that  
44 contained ammonium salts of a range of Hofmeister anions strongly correlated with a reverse  
45 Hofmeister series.<sup>36a</sup> In our experiments, the extent of charging does not correlate with the  
46 Hofmeister series (Figure S3). The proteins should be largely denatured prior to ESI (see below)  
47 and thus, protein structural effects are not expected to significantly affect the extent of analyte  
48 charging in ESI. Collectively, these data were most consistent with acid strength strongly affecting  
49 the extent of protein supercharging in ESI when compared to GB and PA values (of HA and  $A^-$ ),  
50  
51  
52  
53  
54  
55  
56  
57  
58  
59  
60

1 the relative volatility of the acids, and/or the relative extent that  $A^-$  can destabilize protein structures  
2 (Hofmeister effects) under these conditions.  
3

4  
5 *Effects of analyte size.* The effects of acid identity were investigated for carbonic anhydrase  
6 II (CAII) (29 kDa), myoglobin (17 kDa), ubiquitin (8.6 kDa), and angiotensin II (AII; 1,032 Da),  
7 the latter of which should essentially eliminate any tertiary structural effects (Figure 4). For each  
8 analyte, significantly higher analyte charge densities (and significantly less acid adduction) are  
9 formed by use of weak acids than strong acids. For example, addition of any of the 7 weak acids to  
10 solutions containing 4V results in average charges of  $[CAII, zH]^{z+}$  that range from between 43.4  
11 and 40.7 (and average acid adduction of 8.1 to 15.8%), which are an average of 10.8 protons higher  
12 than the average charge states obtained for each of the 5 strong acids (average adduction of 62.7 and  
13 77.6%). By use of weak acids, an average of 7.8, 4.4 and 0.7 more protons ionize myoglobin,  
14 ubiquitin and AII than by use of strong acids. These results indicate that the  $pK_a$  switch at a value of  
15 *ca.* 0 between the formation of relatively high analyte charge densities (and low acid adduction) vs.  
16 low charge densities (and high acid adduction) is a relatively general phenomenon for a reasonably  
17 broad range of analyte sizes (1 to 29 kDa).  
18  
19  
20  
21  
22  
23  
24  
25  
26  
27  
28  
29  
30  
31  
32  
33

34 For ESI solutions that did not contain SCs, the extent of analyte charging did not depend as  
35 strongly on the identity of the acid as those formed from solutions that contained supercharging  
36 additives for CAII, myoglobin, ubiquitin, and AII and the 12 different acids (Figure S4). However,  
37 the extent of acid adduction was significantly higher by use of strong acids than weak acids (Figure  
38 S4). These data indicate that the switch in the extent of acid adduction that occurs at  $pK_a$  values of  
39 *ca.* 0 also occurs for solutions that do not contain SCs (Figure S4) in addition to those that contain  
40 SCs (Figures 3 and 4). In general, the difference in the extent of charging by use of strong compared  
41 to weak acids monotonically increased with as the effectiveness of the solution for enhancing  
42 protein ion charging increased. The relatively minor dependence of the extent of protein ion  
43 charging on acid strength in ESI (no SC additive; Figure S4) can result from the preferential  
44 enrichment of conjugate base anions of strong acids compared to those for weak acids; *i.e.*, the  
45 neutralization of protein ion charge sites by anion binding can counteract the effect of lower  
46  
47  
48  
49  
50  
51  
52  
53  
54  
55  
56  
57  
58  
59  
60

1 solution pH values (and higher anion concentrations) on the extent of protein ion charging in ESI  
2 (with or without SC additives). During the ESI process, the conjugate base anions of strong acids  
3 should be enriched to a greater extent than weak acids to the extent that the proton concentration is  
4 not sufficiently high to neutralize a significant fraction of the anions of strong acids on the timescale  
5 of droplet evaporation, fission, and ion formation (droplet lifetimes of ms to sub-ms).<sup>12a,37</sup>  
6  
7  
8  
9  
10

11 *Effects of gaseous ion conformation(s).* Protonated cytochrome *c* ions were formed in charge  
12 states that ranged from 10 to 25+ depending on the identity of the acid and supercharger (Figure 3),  
13 which corresponds to between 1.0 and 2.4 charge sites per 10 amino acid residues. For ubiquitin,  
14 values of between 1 and 3 charges per 10 amino acid residues were formed under these conditions  
15 (Figure 4). By use of ion-mobility mass spectrometry, Clemmer and co-workers measured the  
16 collisional cross sections of protonated ubiquitin and cytochrome *c* ions that were formed by ESI as  
17 a function of charge state.<sup>5a,b</sup> For ubiquitin and cytochrome *c* ions, compact and partially folded  
18 protein ion structures were formed for the *ca.* 4 to 9+ charge states.<sup>5a,b</sup> For 10+ and higher charge  
19 states, elongated structures were formed. That is, elongated protein ion structures can be formed for  
20 protonated protein ions that have an average of *ca.* 1 or more charges per 10 amino acid residues.  
21 These data suggest that in our experiments, the protein ions should be elongated and any gas-phase  
22 tertiary structural effects on the extent of protein ion charging<sup>5c</sup> should be minimal.  
23  
24  
25  
26  
27  
28  
29  
30  
31  
32  
33  
34  
35  
36  
37

38 For solutions that contain a large fraction of organic protein denaturing solvent (50%  
39 methanol), the use of strong acids also quenches protein supercharging and results in relatively high  
40 acid adduction, whereas the use of weak acids results in the formation of protein ion charge states  
41 with more charge and less acid adduction (Figure 3). For a small peptide (angiotensin II; 1.0 kDa)  
42 that should have minimal tertiary structure, the use of strong acids also resulted in less analyte  
43 charging and more acid adduction than by the use of weak acids (Figure 4). Collectively, these  
44 results indicate that the strong dependence of protein ion charging and acid adduction on the acid  
45 strength is not a result of tertiary gaseous ion conformational effects under these conditions.  
46  
47  
48  
49  
50  
51  
52  
53  
54

55 *Effects of acids on CSD widths.* For the supercharged proteins/peptide ions (cyt *c*, CAII,  
56 myoglobin, ubiquitin), the widths of protein CSDs are relatively narrow for the weak acids and are  
57  
58  
59  
60



1 relatively broad for the strong acids (Figures S5 and S6). For example, the widths of the protonated  
2 CAII CSDs formed from aqueous solutions containing 5  $\mu\text{M}$  CAII, 5% 4V, and 0.5% acid are  
3 significantly higher for the 7 weak acids (the average  $W_z$  value for all 7 weak acids is  $2.3 \pm 0.8$ )  
4 than that for the 5 strong acids (average  $W_z$  value for all 5 strong acids is  $5.2 \pm 0.9$ ). For the other  
5 proteins, the CSDs that are formed from solutions containing weak acids are also broader than those  
6 containing strong acids. For example, the average  $W_z$  values for all strong acids were a respective  
7  $2.7 \pm 0.1$ ,  $4.6 \pm 0.3$ , and  $1.6 \pm 0.2$  for cyt *c*, myoglobin and ubiquitin, which are broader than the  
8 corresponding values for the 7 weak acids ( $1.6 \pm 0.2$ ,  $2.7 \pm 0.4$ , and  $0.8 \pm 0.1$ , respectively); that is,  
9 the use of weak acids narrows the protein ion CSDs by between 40% to 70%. The CSDs were also  
10 wider for the strong acids vs. weak acids for aqueous solutions containing different SCs (Figure  
11 S4). For example, ESI-MS of 5  $\mu\text{M}$  cyt *c*, 0.5% acid (any of the 12 different acids), and 5% of  
12 either 1,4-butanedisulfone, sulfolane, or 1,3-propanedisulfone resulted in an average  $W_z$  value for all 5  
13 strong acids of  $2.8 \pm 0.1$ ,  $2.7 \pm 0.4$ , and  $3.7 \pm 0.9$  vs. the corresponding values of  $2.1 \pm 0.6$ ,  $1.7 \pm$   
14  $0.2$ , and  $2.0 \pm 0.4$  for the 7 weak acids; that is, an average CSD narrowing of 25% to 46% by use of  
15 weak acids compared to strong acids. These data indicate that the binding of conjugate base anions  
16 of acids to protonated protein ions can result in broader protein CSDs and less analyte charging.  
17  
18  
19  
20  
21  
22  
23  
24  
25  
26  
27  
28  
29  
30  
31  
32  
33  
34  
35

36 *Effects of additives on protein structures in solution.* Circular dichroism (CD) spectra were  
37 obtained for aqueous solutions that contained 50  $\mu\text{M}$  cyt *c* with 0.5% acid (or no acid) and between  
38 0 and 9% 4V (Figure 5). For concentrations  $> 9\%$ (v/v), 4V saturated the solution. Generally, the  
39 CD band at *ca.* 194 nm (assigned to the  $\pi \rightarrow \pi^*$  transition of the peptide bond)<sup>38</sup> decreased to less  
40 positive values, as the concentration of 4V increased (Figure 5a), which indicates that the relative  
41 extent of protein disorder increased as the concentration of 4V increased.<sup>38</sup> The CD deconvolution  
42 algorithm (CONTIN) can be used to approximate the relative extent that a protein is unordered by  
43 fitting the CD data (190 to 240 nm) with a linear combination of CD spectra from 16 standard  
44 proteins.<sup>38</sup> Addition of 0.5%(v/v) acetic acid (no 4V) increased the calculated extent of unordered  
45 cyt *c* from *ca.* 10% (aqueous control) to 36% (Figure 5a). In general, the relative extent of  
46 unordered cyt *c* increased from 36% to 68% as the concentration of 4V increased from 0 to  
47  
48  
49  
50  
51  
52  
53  
54  
55  
56  
57  
58  
59  
60

1 9%(v/v), indicating that 4V can denature protein secondary structures in aqueous solutions. These  
2 results (Figure 3 and 5) are consistent with the hypothesis that enrichment of supercharging  
3 additives during the ESI process can chemically denature protein structures and result in more  
4 elongated protein ion conformations that can accommodate higher charge states when formed from  
5 “native” ESI solutions.<sup>22b,39</sup>  
6  
7  
8  
9  
10

11 CD spectra of cyt *c* in aqueous solutions and 1:1 water:methanol that contain 0.5% of each  
12 of the 12 acids were obtained. For both the acidified aqueous and the 1:1 methanol:water solutions,  
13 the CD spectra do not correlate with acid strength for all 12 acids. For example, the CD spectra for  
14 HCOOH ( $pK_a = 3.75$ ) and HI ( $pK_a = -9$ ) are very similar (48.2 and 50.6% unordered, respectively;  
15 Figure 5c). The average calculated extent of unordered protein that is obtained for all 12 acids  
16 increases from  $49.1 \pm 5.5$  % (with 4V) and  $39.5 \pm 4.5$  % (no 4V) for the aqueous solutions to  $83.6 \pm$   
17  $4.4$  % (with 4V) and  $77.3 \pm 4.2$  % (no 4V) for the 1:1 methanol:water solutions, which is consistent  
18 with the addition of methanol denaturing protein secondary structures. Overall, these results  
19 indicate that the strong dependence of protein supercharging in ESI on the use of strong compared  
20 to weak acids (Figures 3 and 4) does not result from (i) differences in the solution-phase protein  
21 structure(s) in solution prior to ESI from either acidified aqueous solutions or acidified  
22 methanol:water solutions and/or (ii) differences in protein denaturation as the composition of the  
23 droplets change owing to preferential evaporation; *i.e.*, the strong dependence of protein ion  
24 supercharging on acid strength does not result from changes in protein ion conformation in solution,  
25 the gas-phase, and during desolvation by use of the different acids.  
26  
27  
28  
29  
30  
31  
32  
33  
34  
35  
36  
37  
38  
39  
40  
41  
42  
43  
44

45 *Mechanism and “effective” pH of ESI droplets.* In our experiments, the initial ESI solutions  
46 prior to ESI contain a significant fraction of water and the pH of the solutions that contain strong  
47 acids are between 1.0 and  $1.2 \pm 0.1$  pH units (*i.e.*, > 99% ionized), while those containing weak  
48 acids are between  $2.6 \pm 0.1$  and  $3.1 \pm 0.1$  pH units (Table 2). The measured pH values do not  
49 significantly change by use of 5%(v/v) 4V (Table 2). From the pH measurements of the ESI  
50 solutions prior to ESI and the Henderson-Hasselbalch equation, the fraction that each acid is ionized  
51 prior to ESI can be obtained (Figure 3a). For the weak acids with  $pK_a$  values that were lower than  
52  
53  
54  
55  
56  
57  
58  
59  
60

1 the pH of the respective solutions, the extent that the acid molecules were ionized prior to ESI were  
2 98%, 97%, and 75% for HIO<sub>3</sub>, H<sub>2</sub>C<sub>2</sub>O<sub>4</sub> and H<sub>3</sub>PO<sub>4</sub>, respectively (Figure 3a). For the weak acids  
3 with pK<sub>a</sub> values greater than the pH of the respective solutions (HCOOH, C<sub>6</sub>H<sub>5</sub>COOH, CH<sub>3</sub>COOH,  
4 C<sub>6</sub>H<sub>5</sub>OH), the extent the acids were ionization prior to ESI were < 10 % (Figure 3a). For ESI, ionic  
5 droplets are preferentially enriched with less volatile solution components (*i.e.*, ions and  
6 supercharging additives)<sup>22b,27</sup> and the relative concentrations of these components should not be at  
7 equilibrium owing to rapid desolvation and droplet fissioning events. For positively charged  
8 droplets formed from acidified solutions, enrichment of H<sub>3</sub>O<sup>+</sup> ions during desolvation can lower the  
9 pH.  
10

11 Because the extent of protein supercharging is significantly higher, acid adduction is  
12 significantly lower, and the CSDs are narrower by use of many different weak acids vs. strong acids  
13 (for many different sizes of proteins/peptides) and because these data do not correlate with proton  
14 affinity, gas-phase basicity, and/or protein conformation (see above), these results suggest that the  
15 charging and supercharging of protein ions in ESI can be significantly limited by the pairing of  
16 conjugate base anions and protonation sites in protein ions. Ion-pairing (*e.g.*, R-NH<sub>2</sub>···H<sup>+</sup>···A<sup>-</sup>  
17 interactions) could occur during ion formation or within the ESI generated droplets prior to the  
18 moment of ion formation. The resulting neutral acid molecules that are non-covalently bound to the  
19 protein ions can be readily lost,<sup>16</sup> which results in the overall loss of one charge from the protein ion  
20 per anion binding event. The anions of strong acids can be preferentially enriched in the droplets  
21 during ESI and the concentration of protons in the resulting droplets may not be sufficiently high to  
22 neutralize a significant fraction the strong acids on the timescale of ESI droplet desolvation and ion  
23 formation (ms to sub-ms)<sup>12a,37</sup> to significantly reduce the extent of ion-pairing (Figure 3). In  
24 contrast, a smaller fraction of the weak acid molecules should be ionized than that for the strong  
25 acids in the ESI droplets upon proton enrichment (Figure 3a), which should reduce the extent that  
26 anions of weak acids neutralize protonation sites during the droplet desolvation and ion formation  
27 processes.  
28  
29  
30  
31  
32  
33  
34  
35  
36  
37  
38  
39  
40  
41  
42  
43  
44  
45  
46  
47  
48  
49  
50  
51  
52  
53  
54  
55  
56  
57  
58  
59  
60

1 Overall, these data suggest that (i) the effective pH values of the droplets that are formed  
2 from solutions containing weak acids are sufficiently lower than the  $pK_a$  values of the acids to  
3 significantly reduce the neutralization of protonation sites on the timescale of droplet desolvation  
4 and ion formation; and (ii) the effective pH values of the droplets that are formed from solutions  
5 that contain strong acids are sufficiently higher than the  $pK_a$  of the acids to result in significant  
6 anion binding to protonated protein ions. The term “effective” is used to acknowledge that these  
7 values were inferred from experimental data for ionic droplets with compositions, sizes, and  
8 temperatures that are not well-defined and rapidly changing; *i.e.*, these values do not correspond to  
9 direct equilibrium measurements. The average and standard deviation of the 8 abscissa inflection  
10 points obtained from the best-fit sigmoid functions in Figures 3 and 4 were  $-0.2$  and  $0.3$ ,  
11 respectively. For the solutions that contain acids with  $pK_a$  values near 0 (nitric, oxalic and iodic  
12 acids), these data indicate that the effective pH values of the ESI generated droplets that result in the  
13 formation of detectable protein ions are near 0 (Figures 3 and 4). The effective pH values obtained  
14 from the inflection points are not significantly affected by the identity (or presence) of SCs for at  
15 least 4 different additives that differ significantly in their effectiveness for supercharging analyte  
16 ions in ESI (Figure 3). In addition, the inflection points are not shifted significantly by the use of  
17 50% methanol (Figure 3). SC additives and methanol may not strongly affect the preferential  
18 enrichment of the conjugate base anions of strong acids ( $> 99\%$  ionized prior to initiating ESI)  
19 during droplet desolvation when formed from solutions that contain a significant fraction of water  
20 under these conditions.

21 Gatlin and Tureček inferred that the pH of relatively neutral water/methanol solutions  
22 decrease by 3-4 pH units based on the dissociation of  $M^{2+}(bpy)_3$ ,  $M = Fe$  and  $Ni$ , in ESI-MS and  
23 solution equilibria calculations.<sup>14</sup> By use of laser-induced fluorescence of a pH sensitive fluorescent  
24 probe molecule in ESI generated droplets, Cook and co-workers determined that the pH of ESI  
25 droplets can decrease by  $\geq 1$  pH unit when formed from near-neutral solutions.<sup>13</sup> The decrease in  
26 the pH of *ca.* 1 to 3 pH units that is inferred from our results (Figures 3 and 4, Table 2) is consistent  
27 with these previous reports.

1 *Effects of solvent.* Mass spectra of [cyt *c*, zH]<sup>z+</sup> were obtained by ESI of solutions containing  
2  
3 5 μM cyt *c*, 5% 4V, 0.5% acetic acid, and 94.5% of either water (GB = 157.7 kcal/mol; γ = 71.99  
4 mN/m), methanol (173.2 kcal/mol; 22.07 mN/m), acetonitrile (179.0 kcal/mol; 28.66 mN/m), or  
5  
6 isopropanol (182.3 kcal/mol; 20.93 mN/m; Figure S7).<sup>33,35</sup> The extent of [cyt *c*, zH]<sup>z+</sup> charging  
7  
8 followed this trend: water (<z> = 22.6 ± 0.2) > methanol (21.7 ± 0.3) ≈ acetonitrile (21.5 ± 0.4) >  
9  
10 isopropanol (20.7 ± 0.3). For solutions that do not contain supercharging additives, the extent of  
11  
12 protein ion charging for three proteins (myoglobin, cytochrome *c*, and ubiquitin) in ESI-MS by use  
13  
14 of solutions that contain 5 μM of protein, 0.5% acetic acid, and no supercharging additive and  
15  
16 99.5% solvent (solvent = methanol, acetonitrile, and isopropyl alcohol) are shown in Figure S8.  
17  
18 High organic solvent concentrations (> 99%) were used to ensure that the mature ionic droplets that  
19  
20 are formed from these solutions in ESI should contain a significant fraction of the organic solvent  
21  
22 and that protein ion conformational effects should be minimal. The extent of cytochrome *c* charging  
23  
24 by use of 99.5% methanol (15.1 ± 0.3), acetonitrile (14.8 ± 0.2) and isopropanol (14.2 ± 0.2) were  
25  
26 the same or slightly decreased as the GB of the solvent increased and surface tension decreased. For  
27  
28 ubiquitin (and myoglobin) and for solutions containing 50/50 water/solvent (solvent = methanol,  
29  
30 acetonitrile, isopropyl alcohol; no supercharger), the same general trends were observed (Figure  
31  
32 S8); *i.e.*, the extent of charging stayed the same or decreased slightly as the GB of the solvent  
33  
34 increased and surface tension decreased. These data are consistent with results for protein ions that  
35  
36 were formed from denaturing solutions that did not contain SCs.<sup>8a</sup> These data suggest that protein  
37  
38 supercharging can be (i) limited by gas-phase proton transfer reactions with solvent molecules<sup>8a</sup> (in  
39  
40 addition to the neutralization of protonation sites by anions within ESI generated droplets); and (ii)  
41  
42 maximised by selecting water in preference to other common ESI solvents. These data are also  
43  
44 consistent with the hypothesis by Williams and co-workers (for denatured protein ions) that higher  
45  
46 droplet surface tension values can result in increased analyte charging.<sup>9a</sup>  
47  
48  
49  
50  
51  
52

53  
54 Loo et al. have proposed that analyte charging can be enhanced by the use of ESI additives  
55  
56 that have conjugate acids (*i.e.*, the protonated additive) that have pK<sub>a</sub> values that are lower than that  
57  
58 of water (< -1.7)<sup>26</sup> and are enriched to a significant extent during the ESI process owing to  
59  
60

1 preferential evaporation. Methanol ( $pK_a = -2$ ; vapour pressure = 127 mmHg), acetonitrile ( $pK_a = -$   
2  
3 10; 88.8 mmHg) and isopropyl alcohol ( $pK_a = -2.2$ ; 45.4 mmHg)<sup>40</sup> all have significantly more  
4  
5 negative  $pK_a$  values for the corresponding conjugate acids ( $SH^+$ ) than protonated water ( $pK_a = -1.7$ )  
6  
7 and these solvents are more volatile than water (23.8 mmHg). Given that (i) acetonitrile has a  $pK_a$   
8  
9 that is 5.0 and 4.5 times lower than methanol and isopropyl alcohol, respectively; (ii) the volatility  
10  
11 of acetonitrile (88 mmHg) is between that of methanol (127 mmHg) and isopropyl alcohol (45.4  
12  
13 mmHg); and (iii) the extent of protein ion charging by use of 99.5% acetonitrile, methanol and  
14  
15 isopropyl alcohol were nearly the same (Figure S8), these data are inconsistent with the hypothesis  
16  
17 that the addition of additives that have low  $pK_a$  values (for the protonated neutral additives;  $SH^+$ )  
18  
19 should necessarily enhance analyte charging.<sup>26</sup> That is, these data are more consistent with analyte  
20  
21 charging being limited by gas-phase proton transfer reactivity<sup>8a</sup> and/or surface tension.<sup>9a</sup>  
22  
23  
24

25 *Improving ion dissociation.* By use of ESI and BC, [ubiquitin, 17H]<sup>17+</sup> can be formed,  
26  
27 readily isolated, and trapped in a 7T FT-ICR MS (Figure S9). Electron capture by [ubiquitin,  
28  
29 17H]<sup>17+</sup> resulted in the formation of an extensive number of relatively non-specific cleavages along  
30  
31 the backbone of the protein ion (*i.e.*, 223 cleavages identified; Figure S10) from which 74 of 75  
32  
33 possible unique inter-residue cleavage sites can be identified (99% sequence coverage). In contrast,  
34  
35 ECD of [ubiquitin, 13H]<sup>13+</sup>, which was the highest charge state that could be isolated without the  
36  
37 use of SC additives, resulted in the identification of 109 cleavages and 44 of 75 inter-residue sites  
38  
39 (59%). In addition, the ECD efficiency and fragmentation efficiency increased significantly from a  
40  
41 respective 79% and 69% for [ubiquitin, 13H]<sup>13+</sup> to 97% and 92% for [ubiquitin, 17H]<sup>17+</sup>.  
42  
43 McLafferty and co-workers reported that by combining data for ECD and collisional activation  
44  
45 dissociation from many charge states (7 to 13+) of ubiquitin, complete sequence can be assigned  
46  
47 (seven charge states).<sup>41</sup> For electron transfer dissociation (ETD) of [ubiquitin, 10H]<sup>10+</sup>, 65 out of 75  
48  
49 unique inter-residue cleavage sites were identified.<sup>42</sup> Here, the identification of 74 of 75 unique  
50  
51 inter-residue cleavage sites corresponds to the highest sequence coverage that has been reported for  
52  
53 a single isolated charge state of ubiquitin by ECD or ETD (to our knowledge).  
54  
55  
56  
57  
58  
59  
60

## Conclusions

1,2-butylene carbonate and 4-vinyl-1,3-dioxalan-2-one can be added to ESI solutions in relatively low concentrations to effectively form protein ions in higher charge states than by use of other known additives and methods. Protein supercharging is significantly more effective by use of water than by use of organic solvents that have high GB values and are commonly used in ESI (*e.g.*, acetonitrile and methanol), indicating that these additives should be avoided to maximize analyte charging. Because these organic solvents are significantly less basic than water in bulk solution, acid/base proton transfer reactions with *neutral* solution additives in ESI generated droplets do not significantly limit analyte charging under these conditions. However, the anions of strong acids ( $pK_a$  values  $< 0$ ;  $> 99\%$  ionized prior to ESI) can effectively quench protein supercharging, broaden protein CSDs, and result in significant acid adduction to protein ions in ESI, whereas weak acids ( $pK_a$  values  $> 0$ ) result in high analyte charge densities, narrow CSDs, and minimal acid adduction, indicating that anion binding can dramatically reduce analyte charging and supercharging in ESI. From these data, the effective pH of ESI generated droplets formed from acidified aqueous protein-denaturing solutions near the moment of ion formation can be near 0, which was between 1 and 3 pH units lower than the solutions from which the ESI droplets were formed. As the effectiveness of supercharging increased for 8 different additives, the protein CSDs narrowed significantly. These results indicate that by discovering even more effective supercharging additives it should be possible to narrow protein ion CSDs further, which should prove beneficial for improving the performance of many MS and tandem-MS measurements. For example, by use of 1,2-butylene carbonate, ESI-MS, and ECD, 99% of all inter-residue amino acid sites can be identified from an ECD mass spectrum of a single isolated charge state of ubiquitin (223 total sequence ions; 92% fragmentation efficiency).

## Acknowledgements

We thank Sydney Liu Lau and Associate Professor Mark Raftery (Bioanalytical MS Facility; BMSF) for helpful discussions. MAZ acknowledges the BMSF for an Honours Research

Scholarship. WAD thanks the Australian Research Council for a Discovery Early Career Research Award fellowship.

### Supplementary Information Available

Tables S1-S5: Effects of ion source voltages and temperatures on the extent of cytochrome *c* charging, SC dipole moment and surface tension values, effects of acid concentration on the CSDs of protonated cytochrome *c*, tune conditions for ESI of different proteins, and acid volatility data. Figure S1-S3: Extent of protonated cytochrome *c* charging plotted vs. GB and PA values of the acids and conjugate base anions of the acids and acid volatility data, and in order of the Hofmeister series. Figures S4-S8: Effects of acid identity on CSDs of proteins/peptides in ESI without SCs, effects of acid identity on the  $W_z$  values for protein ions, and effects of solvent identity on the CSDs for protein ions with and without SCs. Figures S9-S10: ESI and ECD mass spectra and corresponding relative ECD-MS fragment ion abundances at each inter-amino acid residue site for isolated [ubiquitin, 13H]<sup>13+</sup> and [ubiquitin, 17H]<sup>17+</sup>. Full methodological details and an extended discussion of Hofmeister effects are given.

### References

- (1) (a) Fenn, J. B., Mann, M., Meng, C.K., Wong, S.F., and Whitehouse C.M., *Science* **1989**, *24*, 8; (b) Cech, N. B.; Enke, C. G., *Mass. Spectrom. Rev.* **2001**, *20*, 362; (c) Kebarle, P.; Verkerk, U. H., *Mass. Spectrom. Rev.* **2009**, *28*, 898.
- (2) (a) Dongré, A. R., *et al.*, *J. Am. Chem. Soc.* **1996**, *118*, 8365; (b) Tsaprailis, G., *et al.*, *J. Am. Chem. Soc.* **1999**, *121*, 5142; (c) Cerda, B. A., *et al.*, *J. Am. Soc. Mass Spectrom.* **2001**, *12*, 565; (d) Reid, G. E., *et al.*, *Anal. Chem.* **2001**, *73*, 3274; (e) Paizs, B.; Suhai, S., *Mass. Spectrom. Rev.* **2005**, *24*, 508; (f) Flick, T. G.; Donald, W. A.; Williams, E. R., *J. Am. Soc. Mass. Spectrom.* **2013**, *24*, 193; (g) Leeming, M. G., *et al.*, *J. Am. Soc. Mass Spectrom.* **2014**, *25*, 427.
- (3) (a) Zubarev, R. A., *Curr. Opin. Biotechnol.* **2004**, *15*, 12; (b) Cooper, H. J.; Hakansson, K.; Marshall, A. G., *Mass. Spectrom. Rev.* **2005**, *24*, 201; (c) Zubarev, R. A.; Kelleher, N. L.; McLafferty, F. W., *J. Am. Chem. Soc.* **1998**, *120*, 3265; (d) Zubarev, R. A., *et al.*, *Anal. Chem.* **2000**, *72*, 563; (e) Horn, D. M.; Ge, Y.; McLafferty, F. W., *Anal. Chem.* **2000**, *72*, 4778.



- 1  
2  
3  
4  
5  
6  
7  
8  
9  
10  
11  
12  
13  
14  
15  
16  
17  
18  
19  
20  
21  
22  
23  
24  
25  
26  
27  
28  
29  
30  
31  
32  
33  
34  
35  
36  
37  
38  
39  
40  
41  
42  
43  
44  
45  
46  
47  
48  
49  
50  
51  
52  
53  
54  
55  
56  
57  
58  
59  
60
- (4) (a) Zubarev, R. A., *et al.*, *Eur. J. Mass Spectrom.* **2002**, *8*, 337; (b) Donald, W. A., *et al.*, *Proc. Natl. Acad. Sci. U. S. A* **2008**, *105*, 18102; (c) Donald, W. A., *et al.*, *J. Am. Chem. Soc.* **2010**, *132*, 4633; (d) Donald, W. A.; Williams, E. R., *J. Am. Soc. Mass. Spectrom.* **2010**, *21*, 615; (e) Donald, W. A.; Williams, E. R., *Pure Appl. Chem.* **2011**, *83*, 2129.
- (5) (a) Shelimov, K. B., *et al.*, *J. Am. Chem. Soc.* **1997**, *119*, 2240; (b) Valentine, S. J.; Counterman, A. E.; Clemmer, D. E., *J. Am. Soc. Mass. Spectrom.* **1997**, *8*, 954; (c) Konermann, L.; Douglas, D. J., *J. Am. Soc. Mass. Spectrom.* **1998**, *9*, 1248.
- (6) Compton, P. D., *et al.*, *Anal. Chem.* **2011**, *83*, 6868.
- (7) Chowdhury, S. K.; Katta, V.; Chait, B. T., *J. Am. Chem. Soc.* **1990**, *112*, 9012.
- (8) (a) Iavarone, A. T., Jurchen, J.C. and Williams, E.R., *J. Am. Soc. Mass. Spectrom.* **2000**, *11*, 9; (b) Amad, M. H., *et al.*, *J. Mass Spectrom.* **2000**, *35*, 784.
- (9) (a) Iavarone, A. T., and Williams, E.R., *J. Am. Chem. Soc.* **2003**, *125*, 8; (b) Loo, J. A.; Udseth, H. R.; Smith, R. D., *Biol. Mass. Spectrom.* **1988**, *17*, 411.
- (10) Duft, D., *et al.*, *Nature* **2003**, *421*, 128.
- (11) Dole, M., *et al.*, *J. Chem. Phys* **1968**, *49*, 2240.
- (12) (a) Kebarle, P.; Tang, L., *Anal. Chem.* **1993**, *65*, 972A; (b) Iribarne, J. V.; Thomson, B. A., *J. Chem. Phys* **1976**, *64*, 2287; (c) Fernandez de la Mora, J., *Anal. Chim. Acta.* **2000**, *406*, 11.
- (13) Zhou, S.; Prebyl, B. S.; Cook, K. D., *Anal. Chem.* **2002**, *74*, 4885.
- (14) Gatlin, C. L.; Turecek, F., *Anal. Chem.* **1994**, *66*, 712.
- (15) Covey, T. R., *et al.*, *Rapid Commun. Mass Spectrom.* **1988**, *2*, 249.
- (16) Mirza, U. A.; Chait, B. T., *Anal. Chem.* **1994**, *66*, 2898.
- (17) (a) Sterling, H. J., *et al.*, *Anal. Chem.* **2012**, *84*, 3795; (b) Li, Y.; Cole, R. B., *Anal. Chem.* **2003**, *75*, 5739.
- (18) (a) Schnier, P. D.; Gross, D. S.; Williams, E. R., *J. Am. Soc. Mass. Spectrom.* **1995**, *6*, 1086; (b) Schnier, P. D.; Gross, D. S.; Williams, E. R., *J. Am. Chem. Soc.* **1995**, *117*, 6747; (c) Williams, E. R., *J. Mass Spectrom.* **1996**, *31*, 831.

- 1 (19) (a) Chowdhury, S. K., *et al.*, *J. Am. Soc. Mass Spectrom.* **1990**, *1*, 382; (b) Cai, Y.; Cole, R. B.,  
2 *Anal. Chem.* **2002**, *74*, 985; (c) Friess, S. D., *et al.*, *Int. J. Mass Spectrom.* **2002**, *219*, 269; (d) Jiang,  
3 Y.; Cole, R. B., *J. Am. Soc. Mass. Spectrom.* **2005**, *16*, 60; (e) Flick, T. G.; Merenbloom, S. I.;  
4 Williams, E. R., *J. Am. Soc. Mass Spectrom.* **2011**, *22*, 1968.  
5  
6  
7  
8  
9 (20) Krusemark, C. J., *et al.*, *J. Am. Soc. Mass. Spectrom.* **2009**, *20*, 1617.  
10  
11 (21) Kharlamova, A., *et al.*, *Anal. Chem.* **2010**, *82*, 7422.  
12  
13 (22) (a) Lomeli, S. H., *et al.*, *J. Am. Soc. Mass Spectrom.* **2010**, *21*, 127; (b) Sterling, H. J., *et al.*, *J.*  
14 *Am. Soc. Mass Spectrom.* **2011**, *22*, 1178; (c) Iavarone, A. T.; Jurchen, J. C.; Williams, E. R., *Anal.*  
15 *Chem.* **2001**, *73*, 1455; (d) Iavarone, A. T.; Williams, E. R., *Int. J. Mass Spectrom.* **2002**, *219*, 63;  
16 (e) Valeja, S. G., *et al.*, *Anal. Chem.* **2010**, *82*, 7515.  
17  
18 (23) Douglass, K. A.; Venter, A. R., *J. Am. Soc. Mass Spectrom.* **2012**, *23*, 489.  
19  
20 (24) Sze, S. K., *et al.*, *Proc. Natl. Acad. Sci. U. S. A* **2002**, *99*, 1774.  
21  
22 (25) (a) Miladinovic, S. M., *et al.*, *Anal. Chem.* **2012**, *84*, 4647; (b) Meyer, J. G.; Komives, E. A., *J.*  
23 *Am. Soc. Mass. Spectrom.* **2012**, *23*, 1390.  
24  
25 (26) Ogorzalek Loo, R. R.; Lakshmanan, R.; Loo, J. A., *J. Am. Soc. Mass Spectrom.* **2014**, *25*,  
26 1675.  
27  
28 (27) Grimm, R. L.; Beauchamp, J., *J. Phys. Chem. A* **2009**, *114*, 1411.  
29  
30 (28) Samalikova, M., *et al.*, *Anal. Bioanal. Chem.* **2004**, *378*, 1112.  
31  
32 (29) Teo, C. A.; Donald, W. A., *Anal. Chem.* **2014**, *86*, 4455.  
33  
34 (30) Donald, W. A.; Khairallah, G. N.; O'Hair, R. A. J., *J. Am. Soc. Mass Spectrom.* **2013**, *24*, 811.  
35  
36 (31) Graf, M.; García, R. G.; Wätzig, H., *Electrophoresis* **2005**, *26*, 2409.  
37  
38 (32) McLuckey, S. A.; Van Berkel, G. J.; Glish, G. L., *J. Am. Chem. Soc.* **1990**, *112*, 5668.  
39  
40 (33) Haynes, W. M., *CRC Handbook of Chemistry and Physics, 95th Edition*. Taylor & Francis:  
41 2014.  
42  
43 (34) Liu, X.; Cole, R. B., *J. Am. Soc. Mass Spectrom.* **2011**, *22*, 2125.  
44  
45 (35) Hunter, E. P. L.; Lias, S. G., *J. Phys. Chem. Ref. Data.* **1998**, *27*, 413.  
46  
47  
48  
49  
50  
51  
52  
53  
54  
55  
56  
57  
58  
59  
60

- 1 (36) (a) Cassou, C. A.; Williams, E. R., *Anal Chem* **2014**, *86*, 1640; (b) Zhang, Y.; Cremer, P. S.,  
2  
3 *Curr Opin Chem Biol* **2006**, *10*, 658; (c) Hou, M.; Lu, R.; Yu, A., *RSC Advances* **2014**, *4*, 23078.  
4  
5 (37) Mortensen, D. N.; Williams, E. R., *Anal. Chem.* **2014**, *86*, 9315.  
6  
7 (38) Greenfield, N. J., *Nat. Protoc.* **2006**, *1*, 2876.  
8  
9 (39) (a) Sterling, H. J.; Williams, E. R., *J. Am. Soc. Mass Spectrom.* **2009**, *20*, 1933; (b) Hamdy, O.  
10  
11 M.; Julian, R. R., *J. Am. Soc. Mass Spectrom.* **2012**, *23*, 1.  
12  
13 (40) Anslyn, E. V.; Dougherty, D. A., *Modern Physical Organic Chemistry*. University Science:  
14  
15 U.S.A, 2006; pp 259.  
16  
17 (41) Horn, D. M.; Zubarev, R. A.; McLafferty, F. W., *Proc. Natl. Acad. Sci.* **2000**, *97*, 10313.  
18  
19 (42) Sterling, H. J.; Williams, E. R., *Anal. Chem.* **2010**, *82*, 8.  
20  
21  
22  
23  
24  
25  
26  
27  
28  
29  
30  
31  
32  
33  
34  
35  
36  
37  
38  
39  
40  
41  
42  
43  
44  
45  
46  
47  
48  
49  
50  
51  
52  
53  
54  
55  
56  
57  
58  
59  
60

## Tables and Figures

**Table 1.** Performance characteristics of solution additives for increasing the extent of cytochrome *c* and myoglobin charging in ESI-MS.

SC <sup>a</sup>	cytochrome <i>c</i>			myoglobin		
	$z_{\text{HOCS}}/z_{\text{MACS}}$ <sup>b</sup>	$\langle z \rangle^c$	$W_z^d$	$z_{\text{HOCS}}/z_{\text{MACS}}$	$\langle z \rangle$	$W_z$
<b>BC</b>	26/23	22.6(0.2)	1.6(0.2)	34/31	30.6(0.2)	1.7(0.2)
<b>4V</b>	26/23	22.6(0.1)	1.3(0.1)	34/31	30.7(0.1)	1.9(0.1)
<b>PC</b>	25/22	21.8(0.2)	1.4(0.2)	32/30	29.8(0.3)	2.3(0.7)
<b>EC</b>	24/22	21.5(0.2)	2.6(0.1)	–	–	–
<b>BuS</b>	24/22	21.2(0.1)	2.1(0.3)	32/30	29.7(0.4)	3.6(0.9)
<b>Sulf.</b>	23/19	19.4(0.3)	2.9(3.5)	30/28	26.1(0.1)	3.4(0.5)
<b><i>m</i>-NBA</b>	22/18	17.4(0.2)	3.8(2.0)	30/26	24.7(0.6)	4.9(0.8)
<b>PS</b>	22/17	16.5(0.1)	2.9(2.4)	28/22	20.9(0.2)	5.9(1.7)
<b>None</b>	20/15	14.7(0.1)	2.8(1.9)	28/21	20.6(0.5)	6.4(1.3)

<sup>a</sup> 5  $\mu\text{M}$  protein in aqueous solutions containing 0.5% acetic acid. Optimal SC concentrations, % (v/v): 5% BC, 4V, 1,4-butanedisulfone (BuS), and 1,3-propanedisulfone (PS); 30% PC; 10% EC; 3% Sulf. and *m*-NBA. <sup>b</sup>  $z_{\text{HOCS}}/z_{\text{MACS}}$  are the highest observed charge state and the most abundant charge states. <sup>c</sup> Average charge state (standard deviation) of three replicate measurements. <sup>d</sup> Full-width-at-half maximum of Gaussian distributions that are fit to the observed charge state distributions (standard deviation values in parentheses).

**Table 2.** pH values of aqueous solutions containing 0.5% acid (Soln. A), 0.5% acid and 5% 4V (Soln. B), and 0.5% acid, 5% 4V, and 5  $\mu$ M cytochrome *c* (Soln. C).<sup>a</sup>

Acid	Soln. A	Soln. B	Soln. C
HI	1.1	1.1	1.1
HClO <sub>4</sub>	1.2	1.2	1.2
HCl	1.0	1.0	1.0
H <sub>2</sub> SO <sub>4</sub>	1.1	1.1	1.1
HNO <sub>3</sub>	1.1	1.0	1.0
Iodic	2.6	2.6	2.6
Oxalic	2.8	2.8	2.8
H <sub>3</sub> PO <sub>4</sub>	2.7	2.6	2.6
Formic	2.7	2.8	2.8
Benzoic	3.1	3.0	3.0
Acetic	2.9	2.8	2.8
Phenol	3.0	3.1	3.1
No Acid	7.0	7.0	7.0

<sup>a</sup> The standard deviation of three replicate measurements were < 0.1 pH units.

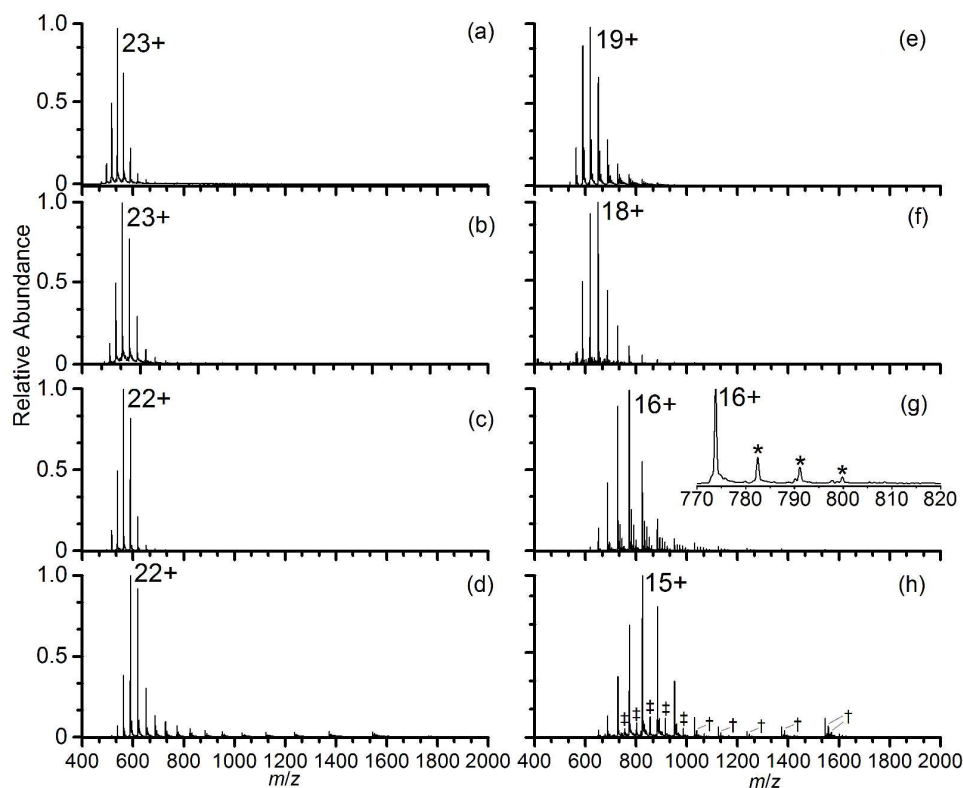


**Figure 1.** Representative electrospray ionization mass spectra of aqueous solutions containing 5  $\mu\text{M}$  cyt *c*, 0.5% (v/v) acetic acid, and (a) 5% 1,2-butylene carbonate, (b) 5% 4-vinyl-1,3-dioxolan-2-one, (c) 30% propylene carbonate, (d) 5% 1,4-butane sultone, (e) 3% sulfolane, (f) 3% *m*-NBA, (g) 5% 1,3-propane sultone, and (h) no supercharging additive. An ion series corresponding to  $[\text{cyt } c, z\text{H}, n(1,3\text{-propane sultone})]^{z+}$  is denoted by “\*”. Adducts correspond to +98 Da (phosphate) are denoted by “†” and chemical noise (12,810 Da; 17+ to 13+) is denoted by “‡”.

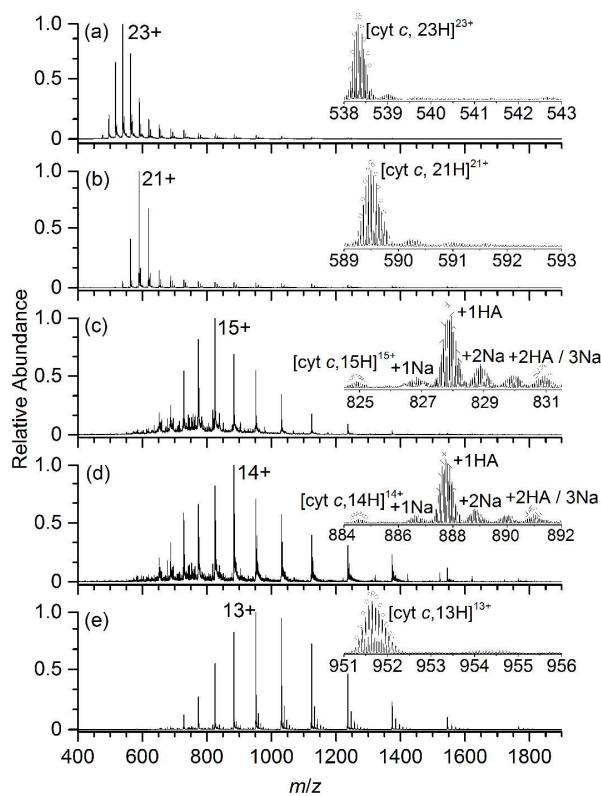


**Figure 2.** ESI LTQ mass spectra of aqueous solutions containing 5  $\mu\text{M}$  *cyt c*, 5% 4V, and 0.5% of either (a) acetic acid, (b) iodic acid, (c) nitric acid, (d) hydroiodic acid, or (e) no acid. Insets are FT-ICR mass spectra of the most abundant protein ion charge states. Theoretical isotope distributions for  $[\text{cyt } c, z\text{H}]^{z+}$  (open circles) and  $[\text{cyt } c, n\text{HA}, z\text{H}]^{z+}$  (crosses; denoted by  $+n\text{HA}$ ) are shown. Ions assigned to  $[\text{cyt } c, n\text{Na}, (z-n)\text{H}]^{(z-n)+}$  are denoted by  $+n\text{Na}$ . For panel (e), an ion series corresponding to  $[\text{cyt } c, z\text{H}, n4\text{V}]^{z+}$  at  $< 25\%$  the most abundant ion  $[\text{cyt } c, 13\text{H}]^{13+}$  was observed.

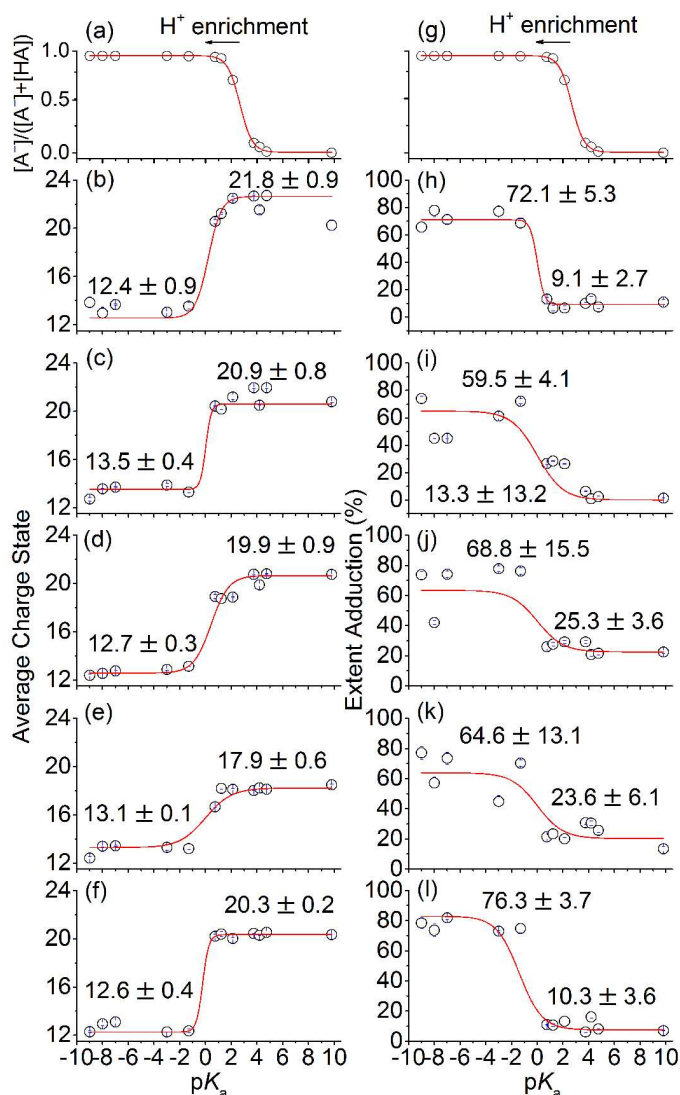


**Figure 3.** The fraction of acid molecules that were ionized ( $HA \rightarrow H^+ + A^-$ ) in solution prior to ESI (a,g). The average charge states of  $[cyt\ c, zH]^{z+}$  (b-f) and extent of acid (HA) adduction (*i.e.*,  $[cyt\ c, nHA, zH]^{z+}$ ; h-l) that were obtained from ESI mass spectra of aqueous solutions containing 5  $\mu$ M *cyt c*, 0.5% acid (HI,  $HClO_4$ , HCl,  $H_2SO_4$ ,  $HNO_3$ ,  $HIO_3$ ,  $H_2C_2O_4$ ,  $H_3PO_4$ , HCOOH,  $C_6H_5COOH$ ,  $CH_3COOH$ ,  $C_6H_5OH$ ), and (b,h) 5% 4V, (c,i) 5% 1,4-butanedisulfone, (d,j) 5% sulfolane, and (e,k) 5% 1,3-propanedisulfone vs. the  $pK_a$  value of the acid. (f,l) The average charge states and extent of acid adduction obtained by use of 5% 4V in 1:1 water:methanol with 0.5% acid vs. acid  $pK_a$  values (*i.e.*, control data for ion conformation effects). For each supercharger, all ESI-MS instrument parameters were kept constant. The average ordinate values of 7 weak acids and 5 strong acids are given.



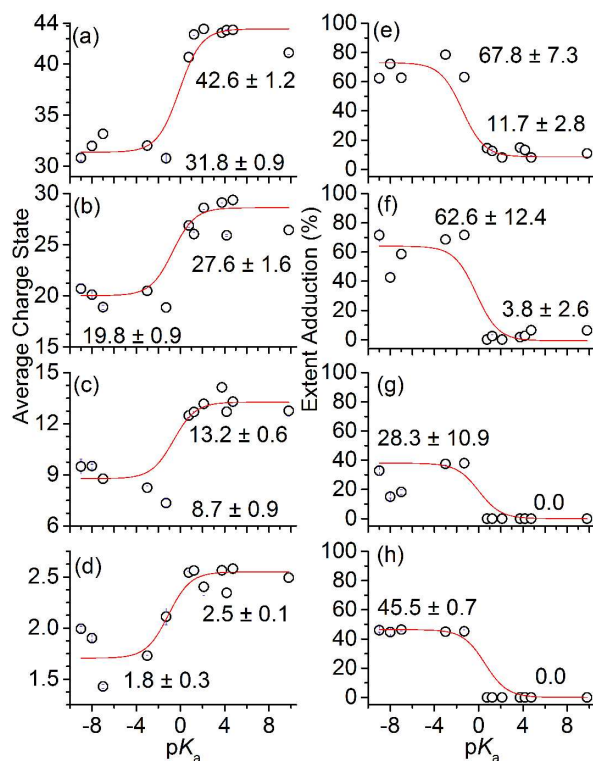


**Figure 4.** The average charge states (a-d) and extent of acid (HA) addition (e-h) that were obtained from ESI mass spectra of aqueous solutions containing 5% 4V, 0.5% acid (same acids as Fig. 2), and (a,e) 5  $\mu$ M CAII, (b,f) 5  $\mu$ M myoglobin, (c,g) 5  $\mu$ M ubiquitin, (d,h) 5  $\mu$ M AII vs. the  $pK_a$  of the acid. For each analyte, all ESI-MS instrument parameters were kept constant. The average ordinate values of 7 weak acids and 5 strong acids are given.

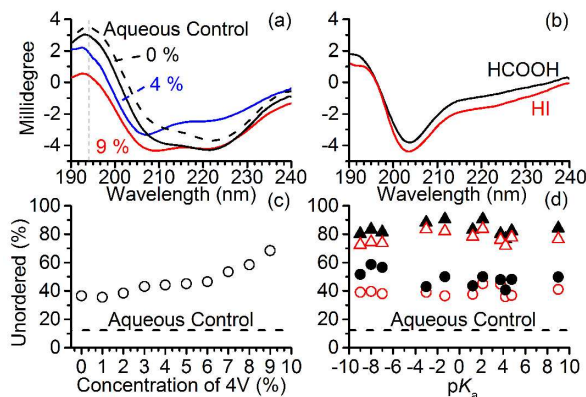


**Figure 5.** (a) Circular dichroism (CD) spectra of 50  $\mu\text{M}$  cyt *c* in aqueous solutions containing 0.5% acetic acid and either 0 (solid black curve), 4 (solid blue curve), or 9% 4V (solid red curve). The CD spectra of the aqueous control (dashed black trace), contains 50  $\mu\text{M}$  cyt *c* (no acid; no supercharging additive). More negative values at 194 nm (grey dashed line) are generally indicative of less ordered protein structure.<sup>38</sup> (b) CD spectra of 50  $\mu\text{M}$  cyt *c* in an aqueous solution that contains 0.5% of either a strong (HI) or weak acid (HCOOH) and no supercharging additive. (c) Relative extent that cyt *c* (50  $\mu\text{M}$ ) is unordered in aqueous solutions that contain 0.5% acetic acid and between 0 and 9% 4V vs. the concentration of 4V. (d) Relative extent that cyt *c* (50  $\mu\text{M}$ ) is unordered in aqueous solutions containing: (i) 0.5% of acid (same acids as in Fig. 2); (ii) either no supercharging additive (open red circles) or 5% -vinyl-1,3-dioxalan-2-one (solid black circles); and (iii) in 1:1 water:methanol containing 0.5% of acid and either no supercharging additive (open red triangles) or 5% 4V (solid black triangles) vs. acid  $\text{p}K_a$  values.